1 # Plant pathogenic bacterium can rapidly evolve tolerance to an antimicrobial plant allelochemical

3 Carrie Louise Alderley[1]# and Ville-Petri Friman[1]

4 [1]University of York, Department of Biology, York, UK

5 Running Head: ITC tolerance in *Ralstonia solanacearum*

6 #Address correspondence to Carrie Louise Alderley, carrie.alderley@york.ac.uk

7 Carrie Louise Alderley and Ville-Petri Friman contributed equally to this work.

8 Abstract word-count: 242

9 Text word-count: 4299

Abstract

Crop losses to plant pathogens are a growing threat to global food security, and hence, more effective control strategies are urgently required. Biofumigation, an agricultural technique, where *Brassica* plant tissues are mulched into soils to release antimicrobial plant allelochemicals called isothiocyanates (ITCs), has been proposed as an environmentally friendly alternative to synthetic agrochemicals. While biofumigation has been shown to suppress a range of plant pathogens, its effects on plant pathogenic bacteria remain largely unexplored. Here we used a laboratory model system to compare the efficacy of different types of ITCs against *Ralstonia solanacearum* plant bacterial pathogen. Additionally, we evaluated the potential for ITC-tolerance evolution under high, intermediate and low transfer frequency ITC exposure treatments. We found that allyl-ITC was the most efficient compound at suppressing *R. solanacearum* growth, and its efficacy was not improved when combined with other types of ITCs. Despite consistent pathogen growth suppression, ITC tolerance evolution was observed in the low transfer frequency exposure treatment. Mechanistically, tolerance was associated with parallel mutations in a gene linked to glucose/sorbonose dehydrogenase, resulting in cross-tolerance to ampicillin beta-lactam antibiotic. Interestingly, pathogen adaptation to the growth media also indirectly selected for increased ITC tolerance through potential metabolic adaptations linked with cell wall structure (serine/threonine kinase) and DNA replication, recombination and repair (deoxyribonucleases). Together, our results suggest that *R. solanacearum* can rapidly evolve tolerance to allyl-ITC plant allelochemical, which could constrain the long-term efficiency of biofumigation biocontrol and potentially shape pathogen evolution with plants.

Keywords: Antimicrobial tolerance, Plant allelochemicals, Rapid evolution, Plant pathogenic bacteria, Biofumigation, Isothiocyanates (ITCs), *Ralstonia solanacearum*

Importance

Several alternatives to agrochemicals have been proposed to reduce crop losses to plant pathogens. One such strategy is called biofumigation, which is a biocontrol technique based on natural plant allelochemicals, such as isothiocyanates (ITCs), that have antimicrobial activity against plant pathogens. Here we show that while one such compound, allyl-ITC, is effective at suppressing the growth of notorious *Ralstonia solanacearum* plant pathogenic bacterium, increased tolerance evolves rapidly, leading to cross-tolerance to the beta-lactam antibiotic, ampicillin. Mechanistically, ITC tolerance was linked to mutations in a putative glucose/sorbonose dehydrogenase gene, which has previously been linked to resistance to clinical antibiotics in other pathogens. Together, our results suggest that plant pathogenic bacteria can rapidly evolve tolerance to antimicrobial compounds produced by plants via similar mechanisms by which they evolve resistance to clinical antibiotics. Potential pathogen tolerance evolution should thus be considered when developing new biocontrol methods based on pathogen growth inhibition.

48 ## Introduction

49 Plant pathogens are a growing threat to global food security, accounting for up to 40% of
50 crop losses annually (1). The phasing out of environmentally toxic chemical fumigants, such
51 as methyl bromide, has directed attention towards alternative biocontrol strategies (2).
52 Plant-derived antimicrobial allelochemicals, such as phenolic acids, terpenes and volatile
53 isothiocyanates (ITCs), are naturally exuded by the roots of legumes (3, 4), cereals (5, 6) and
54 other crops such as *Brassica* (7, 8). These compounds could potentially be used to control
55 pathogens by biofumigation, which involves mulching of plant tissues into soils to release
56 biocidal allelochemicals. While biofumigation has previously been shown to suppress the
57 growth of soil-borne fungal (8–10), nematode (11, 12) and bacterial pathogens (13, 14),
58 outcomes are still varied, ranging from clear pathogen suppression (15, 16) to having no
59 effect (17–19). A better understanding of the antimicrobial and biocidal effects of plant
60 allelochemicals on pathogens is thus required.

61 The success of biofumigation is influenced by various factors including soil
62 conditions, the biofumigant plant species, timing of application and the half-life of biocidal
63 compounds (16). The biocidal effects of *Brassica*-based biofumigation are believed to result
64 primarily from the release of toxic ITCs from their glucosinolate (GSL) pre-cursors (11, 16,
65 20). Moreover, other allelochemicals such as dimethyl sulfide and methyl iodide might
66 contribute to the biocidal activity of biofumigant plants (21, 22). Even though ITC-liberating
67 GSL levels can potentially reach as high as 45.3 mM/m^2 following initial mulching and
68 incorporation of plant material into the soil (23), their concentrations often decline rapidly
69 due to high volatility, sorption to organic matter, leaching from the soil and microbial
70 degradation (16, 24–27). As ITCs often have short half-lives of up to sixty hours (28, 29), it is

71 important to identify ITCs that are highly effective against pathogens even during short-
72 term exposure.

73 The antimicrobial activity of different types of ITCs can vary depending on their
74 mode of action and the species and genotype of the target pathogen. In the case of
75 bacterial pathogens, several antimicrobial mechanisms have been suggested. For instance,
76 ITCs could damage the outer cell membrane of Gram-negative bacteria leading to changes
77 in cell membrane potential (30) and leakage of cell metabolites (31). Further, it has been
78 suggested that ITCs could bind to bacterial enzymes, such as thioredoxin reductases and
79 acetate kinases and disrupt their tertiary structure and functioning (33). It is also possible
80 that some ITCs, such as allyl-ITC, could have multiple targets, making them relatively more
81 toxic to pathogenic bacteria (34). However, antimicrobial activity and potential tolerance
82 evolution to ITCs are still poorly understood in plant pathogenic bacteria.

83 Antibiosis is an important mechanism underlying bacterial competition in soils and
84 soil bacteria often produce and are resistant to several antimicrobials, enabling them to
85 outcompete surrounding bacteria for space and nutrients (35). Antimicrobial tolerance is
86 also important for plant-bacteria interactions, as it can help bacteria to tolerate
87 antimicrobials secreted by plants, such as coumarins, giving them a selective advantage in
88 the plant rhizosphere microbiome (36). Such tolerance has recently been shown to evolve
89 *de novo* in *Pseudomonas protegens* CHA0 bacterium against scopoletin antimicrobial
90 secreted by *Arabidopsis thaliana* (37). Prolonged exposure to plant allelochemicals could
91 thus select for more tolerant plant pathogen genotypes also during biofumigation and will
92 likely be affected by the strength and duration of ITC exposure, which is important in
93 determining whether potential tolerance or resistance mutations have enough time to

94 sweep through pathogen populations. If the mutations enabling ITC tolerance are costly,
95 their selective benefit could be further reduced by competitive trade-offs, leading to loss of
96 tolerance mutations in the absence of ITCs. While ITC concentrations are known to reach
97 antimicrobial levels during biofumigation in the field (8), no direct experimental evidence of
98 ITC tolerance evolution by plant pathogenic bacteria exists.

99 To study these questions, we developed a model laboratory system where we tested
100 the growth-inhibiting effects of ITCs produced by Indian mustard (*Brassica juncea*) on
101 *Ralstonia solanacearum* plant pathogenic bacterium, which is the causative agent of
102 bacterial wilt and potato brown rot diseases. *Ralstonia solanacearum* was chosen as a
103 model species because it is a globally important pathogen, affecting over 200 different plant
104 species including various important crops (38, 39). Furthermore, disease control techniques
105 such as crop rotation, the use of clean and certified seeds or resistant plant cultivars, have
106 shown only limited success in controlling *R. solanacearum* (40–42). Indian mustard (*Brassica*
107 *juncea*) was chosen as a model biofumigant plant due to its well-established allelochemical
108 properties (8, 43–45), which are predominantly caused by the release of allyl, sec-butyl and
109 2-phenylethyl ITCs (46–48). As these ITCs might vary in their biocidal activity, we first tested
110 to what extent they suppress *R. solanacearum* growth when applied either alone or in
111 combination at concentrations relevant to field biofumigation (16, 23, 27, 49, 50).
112 Subsequently, we explored whether long-term exposure to the most effective ITC type could
113 select for resistant or more ITC-tolerant pathogens in the lab, and if ITC tolerance is
114 associated with competitive costs or cross-tolerance to other antimicrobials. It was found
115 that allyl-ITC was the most suppressive allelochemical. However, long-term exposure
116 selected for ITC-tolerant pathogen mutants that also had increased cross-tolerance to the
117 beta-lactam antibiotic ampicillin. No clear competitive costs were observed. Together these

118 results suggest that while Indian mustard could be used as a biofumigant plant against *R.*
119 *solanacearum* due to the high antimicrobial activity of allyl-ITC, its long-term efficacy could
120 be constrained by rapid ITC tolerance evolution.

121 Results

122 (a) Only allyl-ITC suppressed pathogen growth irrespective of the presence of
123 other ITCs

124 We first determined the effects of different ITCs on *R. solanacearum* growth alone and in
125 combination. Overall, there was a significant reduction in *R. solanacearum* densities in the
126 presence of ITCs (ITC presence: $F_{1, 120}$= 6.33, p< 0.01; Tukey: p< 0.05; Fig. 1B). However, this
127 effect was mainly driven by allyl-ITC, which significantly reduced bacterial densities
128 compared to the non-ITC control treatment (ITC type: $F_{7, 114}$= 49.45, p< 0.001; Tukey: p<
129 0.05), while other ITCs had no significant effect on the pathogen (p> 0.05; Fig. 1B).
130 Increasing the ITC concentration from low to high (500 to 1000 μM) had no effect on
131 inhibitory activity in either single or combination ITC treatments (ITC concentration in single
132 ITC treatment: $F_{1, 43}$= 2.0, p= 0.17; combination ITC treatment: $F_{1, 59}$= 0.68, p= 0.41; Fig. 1B).
133 However, a significant interaction between ITC type and ITC concentration in both single
134 and combination treatments was found (ITC concentration x ITC type in single ITC
135 treatment: $F_{2, 39}$= 4.67, p< 0.05; in combination ITC treatment: $F_{3, 53}$= 4.94, p< 0.01; Fig. 1B),
136 which was driven by the increased inhibitory activity of allyl-ITC at high concentration
137 (Tukey: p< 0.05). As a result, ITC combinations were less inhibitory than single ITC
138 treatments (Number of ITCs: $F_{2, 103}$= 3.82, p<0.05; Fig. 1B), which was due to reduced allyl-
139 ITC concentration in combination treatments (total ITC concentrations were kept the same
140 between treatments). Similarly, ITC combinations that included allyl-ITC significantly

141 reduced bacterial densities relative to the control treatment (Allyl-ITC presence: $F_{1, 57}$=
142 36.21, p< 0.001; Fig. 1B), and the presence of allyl-ITC had a clearer effect at the high ITC
143 concentration (Allyl-ITC presence x ITC concentration: $F_{1, 57}$= 7.51, p< 0.01; Fig. 1B). Together
144 these results suggest that allyl-ITC was the most inhibitory ITC and its antimicrobial activity
145 was not enhanced by the presence of other ITCs.

146 (b) Pathogen growth was more clearly suppressed in high and intermediate
147 ITC exposure treatments during an experimental evolution experiment

148 To study the evolutionary effects of ITCs, we exposed the ancestral *R. solanacearum* strain
149 to allyl-ITC at the low concentration (500 μM) and manipulated the frequency of exposure
150 to ITC by transferring a subset of evolved bacterial population to fresh ITC-media mixture
151 everyday (high), every second day (intermediate) and every third day (low) for a total of 16
152 days. As a result, this manipulation also affected the resource renewal rate. Overall, bacteria
153 reached the highest population densities in the low transfer frequency treatments and the
154 second highest in the intermediate transfer frequency treatments (Transfer frequency: $F_{2,}$
155 $_{45}$= 4.66, p< 0.001; p< 0.05 for pairwise comparison; Fig. 2). While allyl-ITC exposure
156 significantly reduced bacterial densities in all ITC-containing treatments (ITC presence: $F_{1, 46}$=
157 30.68, p< 0.001; Fig. 2), bacterial growth was least affected in the low transfer frequency
158 treatment (ITC presence x Transfer frequency: $F_{2, 42}$= 4.36, p< 0.05; p< 0.001 for all pairwise
159 comparisons; Fig. 2). We also observed that the inhibitory activity of allyl-ITC varied over
160 time: while constant suppression was observed in the high and intermediate transfer
161 frequency treatments, pathogen growth suppression became clear in the low transfer
162 frequency treatment only towards the end of the selection experiment potentially due to
163 media growth adaptation in the no-ITC control treatment (Time x Transfer frequency x ITC

164 presence: $F_{2, 673}$= 7.33, p< 0.001; Fig. 2). Together these results suggest that the long-term
165 ITC activity varied temporally and depended on the ITC exposure and serial transfer
166 frequency.

167 (c) ITC tolerance evolution was observed only in the low transfer frequency
168 ITC exposure treatment

169 Fitness assays were conducted at the end of the selection experiment to compare the
170 growth of the ancestral strain and evolved populations from different treatments in the
171 presence and absence of allyl-ITC (experimental concentration: 500 μM). The ancestral
172 strain reached lower densities in the presence of ITC compared to evolved populations
173 regardless of the ITC treatment they had evolved in during the selection experiment
174 (Evolutionary history: $F_{2, 45}$= 5.39, p< 0.01; Tukey: p< 0.05; Fig. 3A). However, ITC tolerance
175 was mainly observed in the low transfer frequency ITC exposure treatment, while
176 populations that had evolved in the high or intermediate transfer frequency treatments did
177 not significantly differ from the ancestral strain (Transfer frequency within ITC-exposed
178 populations: $F_{2, 19}$= 24.72, p< 0.001; Tukey: p< 0.05; Fig. 3A). Surprisingly, even the control
179 populations that had evolved in the absence of ITCs in the low transfer frequency treatment
180 showed an increase in ITC tolerance (p< 0.05; Fig. 3A). One potential explanation for this is
181 that these populations adapted to grow better in CPG media, which could have helped to
182 compensate for the mortality imposed by allyl-ITC during the fitness assays. To test this, we
183 compared the growth of ancestral and evolved populations in the absence of allyl-ITC in the
184 CPG media (Fig. 3B). As expected, all control populations showed improved growth in the
185 CPG media compared to ITC-exposed populations regardless of the transfer frequency
186 treatment (Evolutionary history: $F_{1, 40}$= 20.00, p< 0.001; Transfer frequency: $F_{2, 40}$= 2.66, p=

187 0.08, in all pairwise comparisons, Tukey: $p < 0.05$; Fig. 3B). In contrast, none of the ITC-
188 exposed populations showed improved growth in CPG media relative to the ancestral strain
189 (Tukey: $p < 0.05$; Fig. 3B), which suggests that ITC exposure constrained *R. solanacearum*
190 adaptation to the growth media.

191 To disentangle the effects due to adaptation to the media and allyl-ITC, we repeated
192 fitness assays in 'naïve' LB growth media which the bacteria had not adapted to. ITC
193 tolerance was observed only when bacterial populations had previously been exposed to
194 allyl-ITC (Evolutionary history: $F_{2, 49} = 18.82$, $p < 0.001$; Tukey: $p < 0.05$; Fig. 3C), and this effect
195 was mainly driven by adaptation in the low transfer frequency ITC exposure treatments (no
196 ITC tolerance was observed in the high and intermediate transfer frequency treatment;
197 Transfer frequency: $F_{2, 49} = 4.37$, $p < 0.01$; Tukey: $p < 0.05$; Fig. 3C). Crucially, CPG-adapted
198 control populations showed no signs of ITC tolerance, but instead, suffered reduced growth
199 in LB media relative to the ancestral strain and ITC-exposed populations (Evolutionary
200 history: $F_{2, 49} = 94.89$, $p < 0.001$; Fig. 3D), which was clearest in the low transfer frequency
201 exposure treatment (Evolutionary history x Transfer frequency: $F_{2, 49} = 23.17$, $p < 0.001$; Fig.
202 3D). We further validated our population level fitness results using individual clones (one
203 randomly chosen clone per replicate population per treatment). In line with previous
204 findings, ITC-exposed clones showed increased ITC tolerance compared to the control and
205 ancestral bacterium in the LB media (Evolutionary history: $F_{2, 49} = 14.20$, $p < 0.001$; Fig. 4A),
206 and tolerance evolution was the greatest in the low transfer frequency ITC exposure
207 treatment (Transfer frequency: $F_{2, 49} = 11.15$, $p < 0.001$; Tukey: $p < 0.05$; Evolutionary history x
208 Transfer frequency: $F_{2, 49} = 3.04$, $p < 0.05$; Fig. 4A). Together, our results suggest that ITC
209 tolerance, which evolved in the low transfer frequency ITC exposure treatment was robust
210 and independent of the growth media it was quantified in. Moreover, while all control

211 populations adapted to grow better in the CPG media, this adaptation had a positive effect
212 on ITC tolerance only when quantified in CPG media and when the clones had evolved in the
213 low transfer frequency treatment.

214 (d) Evolution of ITC-tolerance confers cross-tolerance to ampicillin beta-
215 lactam antibiotic

216 To explore potential ITC-tolerance mechanisms, we tested if ITC tolerance correlated with
217 tolerance to ampicillin beta-lactam antibiotic (growth assays), which is commonly produced
218 by various soil bacteria (51). Overall, both low (15 μg/ml) and high (30 μg/ml) ampicillin
219 concentrations had negative effects on *R. solanacearum* growth relative to the no-ampicillin
220 control treatment (Ampicillin concentration: $F_{2, 93}$= 50.12, p< 0.001; Tukey: p< 0.05; high
221 concentration relatively more inhibitory, Fig. S3). However, the evolved clones originating
222 from the low transfer frequency ITC exposure treatment reached significantly higher
223 bacterial densities than the ancestral strain (Evolutionary history: $F_{3, 92}$= 3.51, p< 0.05;
224 Tukey: p< 0.05; Fig. S3), while evolved clones derived from low and intermediate transfer
225 frequency control treatment (no prior ITC exposure) were inhibited to the same extent
226 (Tukey: p> 0.05; Fig. S3). In more detail, ampicillin tolerance in the low transfer frequency
227 clones was only observed under the high ampicillin concentration (Evolutionary history in
228 high ampicillin concentration: $F_{3, 28}$= 8.22, p< 0.001; Fig. S3C), and no improved tolerance
229 was observed under low ampicillin concentration (Evolutionary history in low ampicillin
230 concentration: $F_{3, 28}$= 1.551, p= 0.223; Fig. S3B). Together these results suggest that ITC
231 tolerance conferred cross-tolerance to ampicillin for clones that had evolved in the low
232 transfer frequency ITC exposure treatment.

233 ### (e) ITC tolerance is linked to parallel mutations in a gene encoding
234 ### glucose/sorbonose dehydrogenase

235 A subset of clones which were phenotyped regarding ITC and ampicillin tolerance were
236 selected for genome sequencing (N= 25). Specifically, we focused on comparing parallel
237 mutations between populations that had evolved in the low transfer frequency treatments
238 (clones evolved in the absence and presence of ITC, showing some evidence of tolerance
239 evolution) with ancestral and control populations from the intermediate transfer frequency
240 treatment (no evidence of tolerance evolution). Only a few mutations were observed in 1 to
241 6 different genes, which was expected considering the relatively short duration of the
242 selection experiment (16 days). Of these mutations, 9 were non-synonymous and 4
243 synonymous (Table S2). We mainly focused on comparing differences in parallel non-
244 synonymous mutations and indels which likely have the greatest effect on bacterial
245 phenotypes. Some of these mutations were observed across all treatments, indicative of
246 adaptation to the experimental conditions. For example, parallel non-synonymous
247 mutations in *hisH1* gene controlling imidazole glycerol phosphate synthase were observed
248 in 6/8 to 8/8 replicate clones in all treatments (Fig 5; Table S2). Similarly, non-synonymous
249 mutations in serine/threonine protein kinase genes (between 5/8 to 8/8 replicate clones)
250 and synonymous mutations in putative deoxyribonuclease *RhsC* (between 1/8 to 5/8
251 replicate clones) were found across all treatments (Fig. 5; Table S2). A single clone that had
252 evolved in the absence of allyl-ITC in the intermediate transfer frequency treatment had a
253 unique non-synonymous mutation in the gene encoding the putative HTH-type
254 transcriptional regulator *DmlR* and one other clone originating from this treatment had a
255 mutation in the putative TIS1421-transposase *orfA* protein-encoding gene (Fig. 5; Table S2).
256 Interestingly, one non-synonymous parallel mutation in putative glucose/sorbonose

257 dehydrogenase gene was exclusively identified in all the low transfer frequency ITC
258 exposure clones (present in 8/8 clones; Fig. 5; Table S2) and this gene was also mutated in
259 4/8 replicate clones in the control (no ITC exposure) low transfer frequency treatment
260 (present in 4/8 clones; Fig. 5; Table S2). However, those low transfer frequency control
261 clones possessing the glucose/sorbonose dehydrogenase mutation did not show
262 significantly higher ITC tolerance compared to non-mutated clones when grown in LB
263 supplemented with ITC (the effect of glucose/sorbonose dehydrogenase mutation presence
264 in low transfer frequency control clones: $F_{1, 6}$= 3.05, p= 0.13). This suggests that a
265 combination of mutations may be required for ITC tolerance. Together, these results
266 suggest that bacteria potentially adapted to experimental conditions across all treatments,
267 while ITC tolerance was associated with parallel mutations in the putative
268 glucose/sorbonose dehydrogenase encoding gene.

269 Discussion

270 Here we studied the effects of *Brassica*-derived ITC allelochemicals for the suppression and
271 tolerance evolution of plant pathogenic *R. solanacearum* bacterium in a model
272 biofumigation experiment. We found that only allyl-ITC suppressed *R. solanacearum*
273 growth, while no reduction in pathogen densities were observed when sec-butyl and 2-
274 phenylethyl ITCs were applied alone or in combination. By using experimental evolution, we
275 further show that long-term allyl-ITC exposure selected for ITC tolerance in the low transfer
276 frequency ITC exposure treatment, which was associated with cross-tolerance to ampicillin.
277 At the genetic level, ITC tolerance was linked with parallel mutations in the putative
278 glucose/sorbonose dehydrogenase gene. Together, our results suggest that allyl-ITC derived
279 from Indian mustard is effective at suppressing the growth of the *R. solanacearum* pathogen

280 *in vitro*. However, prolonged exposure could select for increased ITC tolerance, potentially
281 reducing the efficiency of ITC-based biocontrol.

282 Only allyl-ITC suppressed pathogen growth and its effects were not enhanced by the
283 presence of other ITCs. This contradicts previous studies which demonstrated *R.*
284 *solanacearum* sensitivity to 2-phenylethyl ITC at concentrations as low as 330 μM (52).
285 However, in the previous experiment *R. solanacearum* was exposed to 2-phenylethyl ITC in
286 agar instead of liquid media, which has been shown to increase the toxicity of ITCs (8).
287 Moreover, it is possible that different *R. solanacearum* strains respond differently to ITCs,
288 which could also explain discrepancy between ours and other studies. While the suppressive
289 effects of sec-butyl ITC have previously been demonstrated against dust mites (53) and fungi
290 (54), no antimicrobial activity has been observed in bacteria. Variation in the antimicrobial
291 activity of ITCs could be explained by differences in chemical side-chain structure and
292 molecular weight which govern ITC volatility and hydrophobicity (8). Previous studies have
293 shown greater pathogen suppression by ITCs with aliphatic compared to aromatic
294 sidechains in fungal pathogens (8, 55), insect pests (56), and weeds (57). With bacteria, the
295 toxicity of allyl-ITC could be attributed to its high volatility, very short R-side chains and high
296 reactivity (23, 58, 59). These properties could enable rapid diffusion through the liquid
297 media before ITC is lost in the gaseous phase (21). This is supported by a study by Sarwar *et*
298 *al.* (8), where a droplet of aliphatic allyl-ITC was shown to volatilise at room temperature in
299 5 minutes, whilst aromatic 2-phenylethyl ITC remained in the liquid for over 72 hours.
300 Together, our result suggests that high volatility and reactivity could be important
301 properties determining the antibacterial effects of ITCs.

302 The evolution of ITC tolerance was mainly observed in the low transfer frequency ITC
303 exposure treatment. However, we also found that low transfer frequency control
304 populations showed improved tolerance measured in CPG media even though they had not
305 been exposed to allyl-ITC during the experiment. As all treatments were kept separate from
306 each other using tightly sealed bags, this effect is unlikely explained by 'cross selection' due
307 to ITC volatilisation. Alternatively, ITC tolerance evolution could have been linked to certain
308 metabolic adaptations in this transfer frequency treatment. In support of this, we found that
309 evolved control bacterial populations showed improved growth in the CPG media relative to
310 ancestral and ITC-exposed populations, indicative of media adaptation. While similar media
311 adaptations were observed in all control treatment populations, it is not clear why ITC
312 tolerance did not evolve under one- and two-day transfer frequency treatments. One
313 potential explanation for this could be growth-dependent effects on mutation rates. For
314 example, prior studies have shown that bacterial mutation rates can be elevated at
315 stationary phase (60, 61), which could have promoted ITC tolerance and media adaptation
316 in the low transfer frequency treatment where bacteria had spent the relatively longest
317 time at stationary phase (Fig. S1). Alternatively, stationary phase growth conditions could
318 have triggered expression of stress tolerance genes, enabling selection for mutants with
319 relatively higher ITC tolerance (61). For example, expression of *RpoS* sigma factor in *P.*
320 *aeruginosa* has previously been linked to elevated antibiotic resistance and biofilm
321 formation at stationary phase (62, 63). While more work is needed to elucidate these
322 mechanisms, it is likely that the periodic 3-day growth cycle was important for driving ITC
323 tolerance evolution in our experimental conditions. Interestingly, the ITC tolerance that
324 evolved in the absence of allyl-ITC exposure was specific to CPG media and disappeared
325 when measured in 'naïve' LB media. This result suggests that ITC tolerance observed in

326 control populations was likely driven by adaptation to CPG growth media. Such adaptation
327 may have helped to offset the suppressive effects of allyl-ITC by boosting pathogen growth
328 to compensate increased mortality. Alternatively, it is possible that the glucose availability
329 in the CPG media indirectly favoured the evolution of ITC tolerance via metabolic
330 adaptations, which has previously been shown to occur both in the absence (64) and
331 presence of clinical antibiotics (65). Together, our results suggest that prior exposure to
332 allyl-ITC was required for the evolution of robust ITC tolerance, which was independent of
333 the growth media.

334 At the molecular level, ITC tolerance was associated with parallel mutations in a gene
335 predicted to govern glucose/sorbonose dehydrogenase activity. Crucially, all ITC-exposed
336 (8/8) and half of the control clones (4/8) from the low transfer frequency treatment
337 exclusively harboured this mutation. Dehydrogenase enzymes have previously been
338 associated with both metabolism and antibiotic resistance (66, 67). For example, a gain of
339 function mutation in a gene encoding glutamate dehydrogenase has been linked with beta-
340 lactam resistance in *Bacillus subtilis* through altered expression of an extra-cytoplasmic
341 sigma factor (67). Furthermore, in *E. coli*, a mutation in a glucose dehydrogenase gene has
342 been shown to function in lipopolysaccharide modification and calanic acid biosynthesis,
343 which enabled resistance to polymyxin and other antimicrobial peptides (68, 69). These
344 genes have also been linked with beta-lactam resistance in human opportunistic
345 *Staphylococcus aureus* pathogen through increased cell wall thickness and reduced cell wall
346 antibiotic permeability (70). In line with this, we found that ITC tolerance conferred cross-
347 tolerance to ampicillin beta-lactam antibiotic in clones originating from the low transfer
348 frequency ITC exposure treatment. However, the glucose/sorbonose dehydrogenase did not
349 confer increased tolerance for clones that had evolved in low transfer frequency control

350 treatment in the absence of allyl-ITC. This suggests that other mutations might have also
351 been important for ITC tolerance via potential epistatic interactions.

352 Three clones from the intermediate transfer frequency transfer treatment had unique
353 mutations in a gene encoding a probable transcription regulator protein. While there is little
354 information available regarding this gene, it is located beside the IS2 transposase *TnpB*
355 gene, potentially affecting its regulation in DNA replication, recombination and repair
356 activity (71). In addition, we observed mutations in genes encoding putative
357 serine/threonine protein kinases, amino acid biosynthesis (*hisH1* gene) and DNA replication,
358 recombination and repair (putative *RhsC* gene) in clones from all treatments. While more
359 work is required to directly test the role of these mutations, they were likely associated with
360 bacterial growth and metabolism, which could have resulted from adaptation to the growth
361 media during the selection experiment. Accumulating evidence suggests that antimicrobial
362 resistance can be indirectly driven by metabolic adaptations (72) and through stepwise
363 accumulation of multiple mutations that confer high-level antibiotic resistance via epistasis
364 (73, 74). While little is known about ITC tolerance mechanism in bacteria, it has previously
365 been shown that upregulation of three glutathione S-transferase encoding genes (linked to
366 protecting cells from oxidative damage) (75) were required for the induction of ITC
367 tolerance in the stem rot fungal plant pathogen *Sclerotinia sclerotiorum* (76). Concurrently,
368 mutations observed in serine/threonine protein kinase genes could have potentially
369 affected ITC tolerance if these enzymes were targeted by the ITCs as has been shown before
370 in the fungus *Alternaria brassicicola* (77), and bacterial pathogen *Escherichia coli* (34). It
371 would also be interesting to study potential trade-offs between tolerance and other
372 pathogen life-history traits in the future. While we did not observe clear growth costs
373 associated with ITC tolerance, mutations in dehydrogenase genes have previously been

374 associated with loss of virulence in *R. solanacearum* (78). Such trade-offs could potentially
375 counteract the drawbacks of tolerance evolution by constraining disease outbreaks through
376 reduced virulence.

377 In conclusion, our findings demonstrate that allyl-ITC could potentially be used to
378 suppress the growth of *R. solanacearum* plant pathogen. However, repeated ITC exposure
379 could select for mutants with increased ITC tolerance, potentially weakening the long-term
380 efficiency of ITCs and biofumigation. Future work should focus on validating these findings
381 in more complex natural environments. For example, it is currently not clear if *R.*
382 *solanacearum* ITC tolerance evolves in the plant rhizosphere in the presence of other
383 microbes that could constrain mutation supply rate via resource and direct competition.
384 Moreover, different resistance mechanisms could be selected depending on soil
385 physiochemical properties and nutrient and plant root exudate availability. Furthermore, it
386 is not clear if the ITC concentrations used in this experiment are achievable through
387 biofumigation and whether they would have negative effects also on beneficial soil
388 microbes. More efficient ITC application could be attained by drilling the biofumigant plants
389 into fields at the time of flowering when GSL levels are the highest using finely chopped
390 plant material, which maximises cell disruption and ITC release to the soil (79). In addition,
391 the efficacy of *Brassica*-based biofumigation could potentially be improved by using plant
392 cultivars with elevated levels of sinigrin, the GSL precursor to allyl-ITC. Comprehensive *in*
393 *vivo* work is thus required to validate the potential of allyl-ITC for *R. solanacearum*
394 biocontrol in the field.

395 Materials and Methods

396 (a) Pathogen strain and culture media

397 We used a *Ralstonia solanacearum* strain which was originally isolated from the river
398 Loddon (phylotype II sequevar 1) in the UK as our pathogen strain (Source: John
399 Elphinstone, Fera Science, 2014). This strain was chosen as river water is the most common
400 environmental source of potato brown rot outbreaks in the UK (Elphinstone *et al*., 1998),
401 and hence highly relevant for UK *R. solanacearum* epidemics. The strain was cultured in CPG
402 broth (1 g casamino acids, 10 g peptone and 5 g glucose per litre of ddH_2O) for 48 hours at
403 28 °C to create cryostocks (20% w/v glycerol) that were preserved at -80 °C. CPG was also
404 used as the main growth media in all experiments except for fitness assays, where lysogeny
405 broth (LB: 10 g tryptone, 5 g yeast, 10 g NaCl per litre of ddH_2O) was also used as a 'naïve'
406 growth media to control the effects of *R. solanacearum* adaptation to CPG media during the
407 selection experiment.

408 **(b) Comparing the effects of different types of ITCs for pathogen suppression**

409 To determine antimicrobial activity of ITCs, we first identified concentrations that caused a
410 significant reduction in *R. solanacearum* growth relative to the non-ITC exposed control
411 treatments. To this end, we conducted short-term growth assays where *R. solanacearum*
412 was exposed to allyl, sec-butyl and 2-phenylethyl ITCs at 63, 125, 250, 500, 1000, 2500 and
413 5000 μM concentrations in CPG media (Fig. S2). For this experiment, *R. solanacearum* was
414 revived from cryostocks by growing with shaking (250 rpm) for 48 hours at 28 °C before
415 normalising bacterial density to an optical density (OD) reading of 0.1 (600 nm; Tecan,
416 Sunrise), equalling ~10^7 cells per ml. This method was consistently used to revive and adjust
417 bacterial densities in all growth experiments. *R. solanacearum* was grown in 200 μl CPG
418 media in different ITC concentrations for 148 hours and bacterial densities were measured
419 every 24 hours as optical density (OD) at 600 nm. We found that allyl-ITC concentrations as

420 low as 125 μM inhibited *R. solanacearum* growth, while relatively higher concentrations of
421 500 μM of sec-butyl and 2-phenylethyl ITC were required to inhibit pathogen growth (Fig.
422 S2). Based on this data, 500 μM and 1000 μM ITC concentrations were selected because
423 they showed pathogen growth suppression in the case of all measured ITCs (Table S1).
424 Furthermore, these concentrations are known to be achievable at least transiently during
425 biofumigation in the field (16, 23, 27, 50, 80). To explore the effects of ITCs on pathogen
426 growth alone and in combination, different ITCs were mixed in all possible two-way and
427 three-way combinations using equal concentrations of each ITC within combinations (two-
428 way 50:50%; three-way 33:33:33%) to achieve final low (500 μM) and high (1000 μM) ITC
429 concentrations in 200 μl of CPG media in 96-well microplates. Microplates were cultured at
430 28 °C (N= 8) and the experiment was run for three days (72 hours), with population density
431 measurements recorded every 24 hours as optical density at 600 nm.

432 (c) Determining pathogen ITC and beta-lactam tolerance evolution in response
433 to repeated allyl-ITC exposure

434 To investigate the potential for ITC tolerance evolution, we set up a 16-day selection
435 experiment where we exposed *R. solanacearum* to 500 μM of allyl-ITC, which has the
436 strongest effect on pathogen growth suppression of all tested ITCs (Fig. 1A; Fig. S2). We also
437 manipulated the frequency of ITC exposure using high (1-day), intermediate (2-day) and low
438 (3-day) serial transfer frequency treatments. At each serial transfer, a subset of evolved
439 bacteria (5% of the homogenised bacterial population) was subcultured to fresh CPG media
440 in the absence (control) and presence of allyl-ITC. ITC treatments thus manipulated both
441 resource renewal and exposure to fresh ITCs. The selection experiment was set-up following
442 the same protocols described earlier and following this, separate fitness assays were

443 conducted to directly compare the growth of ancestral and evolved populations (and
444 individual colonies) in the absence and presence of 500 μM allyl-ITC. In addition to testing
445 potential ITC tolerance evolution, we quantified the potential costs of ITC tolerance and
446 adaptation to the growth media (CPG) by growing the strains in the absence of ITCs. All
447 fitness assays were also repeated in 'naïve' LB media to control the potential effects of
448 pathogen adaptation to the CPG growth media during the selection experiment. In all
449 assays, bacteria were revived and prepared as described earlier, and grown in 96-well
450 microplates in different media (CPG or LB) in the absence or presence of 500 μM allyl-ITC for
451 72 hours. Changes in ITC tolerance were quantified as bacterial growth relative to the
452 ancestral and control treatments based on optical density at 600 nm (48-hour time point).
453 Fitness assays were also conducted for individual bacterial colonies at the final time point
454 where a single ancestral colony and one colony from each replicate selection line per
455 treatment were selected resulting in a total of 49 clones. We also measured if ITC exposure
456 led to cross-tolerance to the beta-lactam antibiotic ampicillin, using the sequenced isolated
457 clones from the final time point of the selection experiment (intermediate transfer
458 frequency no-ITC, low transfer frequency no-ITC and low transfer frequency ITC exposure
459 treatments) and the ancestral strain (total of 24 evolved clones and 8 replicate ancestral
460 clones). Clones were prepared as described earlier and grown in 96-well microplates in CPG
461 media in the absence or presence of 15 or 30 μg/ml ampicillin. Ampicillin tolerance was
462 quantified as bacterial growth relative to the ancestral clones based on optical density at
463 600nm (48-hour time point).

464 **(d) Genome sequencing of evolved bacterial clones**

465 A subset of evolved clones was whole genome sequenced (Illumina 30x coverage) to identify
466 potential single nucleotide polymorphisms (SNPs) and genomic rearrangements (small

467 insertions and deletions) linked with *R. solanacearum* adaptation. Based on phenotypic
468 data, we chose eight clones (1 per replicate selection line) from the low transfer frequency
469 treatments that had evolved in the absence or presence of ITC (16 clones), the ancestral
470 strain (1 clone), and as a control, eight clones from the intermediate transfer frequency no-
471 ITC treatment (8 clones) that showed no evidence of ITC tolerance adaptation (a total of 25
472 clones). Genomic DNA was extracted using the Qiagen DNeasy UltraClean Microbial Kit
473 according to the manufacturer's protocol. DNA was quantified using the NanoDrop
474 microvolume spectrophotometer and quality checked by gel electrophoresis imaging. DNA
475 yields of all samples were diluted with EB buffer to 30 ng/μl concentrations and DNA
476 samples were sent to MicrobesNG for sequencing (http://www.microbesng.uk).
477 MicrobesNG conducted library preparation using Nextera XT Library Prep Kit (Illumina, San
478 Diego, USA) following the manufacturer's protocol with the following modifications: 2 ng of
479 DNA were used as input, and PCR elongation lasted 1 min. Hamilton Microlab STAR
480 automated liquid handling system was used for DNA quantification and library preparation.
481 Pooled libraries were quantified using the Kapa Biosystems Library Quantification Kit for
482 Illumina on a Roche light cycler 96 qPCR machine. Libraries were sequenced on the Illumina
483 HiSeq 2500 using a 250 bp paired end protocol. Reads were adapter trimmed using
484 Trimmomatic 0.30 with a sliding window quality cut-off of Q15 (Bolger *et al*., 2014).
485 Assembly was performed on samples using SPAdes version 3.7 (Bankevich *et al*., 2012) and
486 contigs were annotated using Prokka 1.11 (81). Genomes were analysed using a standard
487 analysis pipeline, where reads were first mapped to a high quality and well annotated
488 UY031 reference genome (82) which showed 99.95% similarity with our *R. solanacearum*
489 strain at the chromosome level and 97.87% similarity at the mega-plasmid level. Variant
490 calling was performed using Snippy, a rapid haploid variant calling pipeline (Snippy v3.2).

491 When comparing the sequenced genomes, the SNPs identified in both the ancestral strain
492 and the evolved clones were first filtered out as these likely represent pre-existing
493 phylogenetic differences between the reference genome and our ancestral *R. solanacearum*
494 strain. We also compared the control treatment clones isolated from low and intermediate
495 transfer frequency treatments (no ITC exposure) to identify potential mutations linked with
496 CPG media adaptation. Additionally, we used phage identification software Phaster (83),
497 and mobile genetic element integration identification software MGEfinder (84) to identify
498 potential phenotypic changes via mobile genetic elements but did not observe any clear
499 differences between ITC-exposure treatments. All genomes including the ancestral strain
500 have been deposited in the European Nucleotide Archive database under the following
501 accession number: PRJEB42551.

502 **(e) Statistical analysis**

503 Repeated measures ANOVA was performed to analyse all the data with temporal sampling
504 structure and pairwise differences were determined using *post-hoc* t-test with Bonferroni
505 correction. All other statistical analyses (ITC tolerance and cost of tolerance in CPG and LB
506 media and cross-tolerance in ampicillin) were conducted focusing on the 48-hour
507 measurement time point (where ITC was still actively suppressive to *R. solanacearum,* Fig.
508 S1) and two-way ANOVA was used to explain variation in bacterial growth between different
509 treatments. Tukey *post-hoc* tests were used to compare differences between subgroups ($p<$
510 0.05). Where data did not meet the assumptions of a parametric test, non-parametric
511 Kruskal-Wallis test and *post-hoc* Dunn test were used. All statistical analyses and graphs
512 were produced using R (R Foundation for Statistical Computing, R Studio Version (3. 5. 1),
513 Packages: ggplot, tidyverse, ggpubr, lme4, rcompanion).

Acknowledgements

This work was funded by the NERC ACCE DTP (CA), the Royal Society (RSG\R1\180213 and CHL\R1\180031; V-P.F) and jointly by a grant from UKRI, Defra, and the Scottish Government, under the Strategic Priorities Fund Plant Bacterial Diseases programme (BB/T010606/1; V-P.F) at the University of York. The funders had no role in study design, data collection and interpretation, or the decision to submit the work for publication.

520 # References

521 1. Savary S, Ficke A, Aubertot JN, Hollier C. 2012. Crop losses due to diseases and their
522 implications for global food production losses and food security. Food Secur. Springer.

523 2. Handbook for the International Treaties for the Protection of the Ozone ... - United Nations
524 Environment Programme - Google Books.

525 3. Wink M. 2013. Evolution of secondary metabolites in legumes (Fabaceae). South African J Bot
526 89:164–175.

527 4. Mondal MF, Asaduzzaman M, Asao T. 2015. Adverse Effects of Allelopathy from Legume
528 Crops and Its Possible Avoidance. Am J Plant Sci 06:804–810.

529 5. Mazzola M, Gu YH. 2002. Wheat genotype-specific induction of soil microbial communities
530 suppressive to disease incited by Rhizoctonia solani Anastomosis Group (AG)-5 and AG-8.
531 Phytopathology 92:1300–1307.

532 6. Larkin RP, Halloran JM. 2015. Management effects of disease-suppressive rotation crops on
533 potato yield and soilborne disease and their economic implications in potato production. Am
534 J Potato Res 91:429–439.

535 7. Kirkegaard JA, Wong PTW, Desmarchelier JM. 1996. In vitro suppression of fungal root
536 pathogens of cereals by Brassica tissues. Plant Pathol 45:593–603.

537 8. Sarwar M, Kirkegaard JA, Wong PTW, Desmarchelier JM. 1998. Biofumigation potential of
538 brassicas. Plant Soil 201:103–112.

539 9. Angus JF, Gardner PA, Kirkegaard JA, Desmarchelier JM. 1994. Biofumigation: Isothiocyanates
540 released frombrassica roots inhibit growth of the take-all fungus. Plant Soil 162:107–112.

541 10. Rumberger A, Marschner P. 2003. 2-Phenylethylisothiocyanate concentration and microbial
542 community composition in the rhizosphere of canola. Soil Biol Biochem 35:445–452.

543 11. Lord JS, Lazzeri L, Atkinson HJ, Urwin PE. 2011. Biofumigation for Control of Pale Potato Cyst
544 Nematodes: Activity of Brassica Leaf Extracts and Green Manures on Globodera pallida in
545 Vitro and in Soil. J Agric Food Chem 59:7882–7890.

546 12. Ngala BM, Woods SR, Back MA. 2015. Sinigrin degradation and G. pallida suppression in soil
547 cultivated with brassicas under controlled environmental conditions. Appl Soil Ecol 95:9–14.

548 13. Ji P, Momol MT, Rich JR, Olson SM, Jones JB. 2007. Development of an Integrated Approach
549 for Managing Bacterial Wilt and Root-Knot on Tomato Under Field Conditions. Plant Dis
550 91:1321–1326.

551 14. Hu P, Hollister EB, Somenahally AC, Hons FM, Gentry TJ. 2015. Soil bacterial and fungal
552 communities respond differently to various isothiocyanates added for biofumigation. Front
553 Microbiol 5:729.

554 15. Larkin RP, Griffin TS. 2007. Control of soilborne potato diseases using Brassica green
555 manures. Crop Prot 26:1067–1077.

556 16. Matthiessen JN, Kirkegaard JA. 2006. Biofumigation and Enhanced Biodegradation:
557 Opportunity and Challenge in Soilborne Pest and Disease Management. CRC Crit Rev Plant Sci
558 25:235–265.

559 17. Kirkegaard JA, Sarwar M, Wong PTW, Mead A, Howe G, Newell M. 2000. Field studies on the

560 biofumigation of take-all by Brassica break crops. Aust J Agric Res 51:445–456.

561 18. Stirling GR, Stirling AM. 2003. The potential of Brassica green manure crops for controlling
562 root-knot nematode (Meloidogyne javanica) on horticultural crops in a subtropical
563 environment. Aust J Exp Agric 43:623–630.

564 19. Hartz TK, Johnstone PR, Miyao EM, Davis RM. 2005. Mustard cover crops are ineffective in
565 suppressing soilborne disease or improving processing tomato yield. HortScience 40:2016–
566 2019.

567 20. Gimsing AL, Kirkegaard JA. 2009. Glucosinolates and biofumigation: fate of glucosinolates and
568 their hydrolysis products in soil. Phytochem Rev 8:299–310.

569 21. Wang D, Rosen C, Kinkel L, Cao A, Tharayil N, Gerik J. 2009. Production of methyl sulfide and
570 dimethyl disulfide from soil-incorporated plant materials and implications for controlling
571 soilborne pathogens. Plant Soil 324:185–197.

572 22. Vervoort MTW, Vonk JA, Brolsma KM, Schütze W, Quist CW, De Goede RGM, Hoffland E,
573 Bakker J, Mulder C, Hallmann J, Helder J. 2014. Release of isothiocyanates does not explain
574 the effects of biofumigation with Indian mustard cultivars on nematode assemblages. Soil
575 Biol Biochem 68:200–207.

576 23. Kirkegaard JA, Sarwar M. 1998. Biofumigation potential of brassicas: I. Variation in
577 glucosinolate profiles of diverse field-grown brassicas. Plant Soil 201:71–89.

578 24. Frick A, Zebarth BJ, Szeto SY. 1998. Behavior of the Soil Fumigant Methyl Isothiocyanate in
579 Repacked Soil Columns. J Environ Qual 27:1158–1169.

580 25. Warton B, Matthiessen JN, Shackleton MA. 2001. Glucosinolate content and isothiocyanate
581 evolution - Two measures of the biofumigation potential of plants. J Agric Food Chem
582 49:5244–5250.

583 26. Hanschen FS, Yim B, Winkelmann T, Smalla K, Schreiner M. 2015. Degradation of Biofumigant
584 Isothiocyanates and Allyl Glucosinolate in Soil and Their Effects on the Microbial Community
585 Composition. PLoS One 10:e0132931.

586 27. Gimsing AL, Poulsen JL, Pedersen HL, Hansen HCB. 2007. Formation and degradation kinetics
587 of the biofumigant benzyl isothiocyanate in soil. Environ Sci Technol 41:4271–4276.

588 28. Borek V, Morra MJ, Brown PD, McCaffrey JP. 1995. Transformation of the Glucosinolate-
589 Derived Allelochemicals Allyl Isothiocyanate and Allylnitrile in Soil. J Agric Food Chem
590 43:1935–1940.

591 29. Gimsing AL, Kirkegaard JA. 2006. Glucosinolate and isothiocyanate concentration in soil
592 following incorporation of Brassica biofumigants. Soil Biol Biochem 38:2255–2264.

593 30. Sofrata A, Santangelo EM, Azeem M, Borg-Karlson A-K, Gustafsson A, Pütsep K. 2011. Benzyl
594 Isothiocyanate, a Major Component from the Roots of Salvadora Persica Is Highly Active
595 against Gram-Negative Bacteria. PLoS One 6:e23045.

596 31. Lin C-M, Preston Iii JF, Wei C-I. 2000. Antibacterial Mechanism of Allyl Isothiocyanate. J Food
597 Prot 63:727–734.

598 32. BROWN, D. P. 1997. Control of soil-borne plant pests using glucosinolate-containing plants.
599 Adv Agron 61:168–231.

600 33. Luciano FB, Holley RA. 2009. Enzymatic inhibition by allyl isothiocyanate and factors affecting
601 its antimicrobial action against Escherichia coli O157:H7. Int J Food Microbiol

602 https://doi.org/10.1016/j.ijfoodmicro.2009.03.005.

603 34. Luciano FB, Holley RA. 2009. Enzymatic inhibition by allyl isothiocyanate and factors affecting
604 its antimicrobial action against Escherichia coli O157:H7. Int J Food Microbiol 131:240–245.

605 35. Hibbing ME, Fuqua C, Parsek MR, Peterson SB. 2010. Bacterial competition: Surviving and
606 thriving in the microbial jungle. Nat Rev Microbiol. Nature Publishing Group.

607 36. Stringlis IA, Yu K, Feussner K, De Jonge R, Van Bentum S, Van Verk MC, Berendsen RL, Bakker
608 PAHM, Feussner I, Pieterse CMJ. 2018. MYB72-dependent coumarin exudation shapes root
609 microbiome assembly to promote plant health. Proc Natl Acad Sci U S A 115:E5213–E5222.

610 37. Li E, de Jonge R, Liu C, Jiang H, Friman VP, Pieterse CMJ, Bakker PAHM, Jousset A. 2020. Rapid
611 evolution of bacterial mutualism in the plant rhizosphere. bioRxiv. bioRxiv.

612 38. Yabuuchi E, Kosako Y, Yano I, Hotta H, Nishiuchi Y. 1995. Transfer of Two *Burkholderia* and An
613 *Alcaligenes* Species to *Ralstonia* Gen. Nov. Microbiol Immunol 39:897–904.

614 39. Elphinstone JG. 2005. The current bacterial wilt situation: a global overview. Bact wilt Dis
615 Ralstonia solanacearum species complex 9–28.

616 40. Ciampi-Panno L, Fernandez C, Bustamante P, Andrade N, Ojeda S, Contreras A. 1989.
617 Biological control of bacterial wilt of potatoes caused byPseudomonas solanacearum. Am
618 Potato J 66:315–332.

619 41. Ramesh R, Joshi AA, Ghanekar MP. 2009. Pseudomonads: major antagonistic endophytic
620 bacteria to suppress bacterial wilt pathogen, Ralstonia solanacearum in the eggplant
621 (Solanum melongena L.). World J Microbiol Biotechnol 25:47–55.

622 42. Chellemi DO, Olson SM, Mitchell DJ, Secker I, McSorley R. 1997. Adaptation of soil
623 solarization to the integrated management of soilborne pests of tomato under humid
624 conditions. Phytopathology 87:250–258.

625 43. Bending GD, Lincoln SD. 1999. Characterisation of volatile sulphur-containing compounds
626 produced during decomposition of Brassica juncea tissues in soil. Soil Biol Biochem 31:695–
627 703.

628 44. Mazzola M, Hewavitharana SS, Strauss SL. 2015. *Brassica* Seed Meal Soil Amendments
629 Transform the Rhizosphere Microbiome and Improve Apple Production Through Resistance
630 to Pathogen Reinfestation. Phytopathology 105:460–469.

631 45. Kirkegaard JA, Matthiessen JN. 2005. Developing and refining the biofumigation concept.

632 46. Olivier C, Vaughn SF, Mizubuti ESG, Loria R. 1999. Variation in allyl isothiocyanate production
633 within Brassica species and correlation with fungicidal activity. J Chem Ecol 25:2687–2701.

634 47. Bangarwa SK, Norsworthy JK, Mattice JD, Gbur EE. 2011. Glucosinolate and Isothiocyanate
635 Production from Brassicaceae Cover Crops in a Plasticulture Production System. Weed Sci
636 59:247–254.

637 48. Yim B, Hanschen FS, Wrede A, Nitt H, Schreiner M, Smalla K, Winkelmann T. 2016. Effects of
638 biofumigation using Brassica juncea and Raphanus sativus in comparison to disinfection using
639 Basamid on apple plant growth and soil microbial communities at three field sites with
640 replant disease. Plant Soil 406:389–408.

641 49. Hanschen FS, Brüggemann N, Brodehl A, Mewis I, Schreiner M, Rohn S, Kroh LW. 2012.
642 Characterization of products from the reaction of glucosinolate-derived isothiocyanates with
643 cysteine and lysine derivatives formed in either model systems or broccoli sprouts. J Agric

644 Food Chem 60:7735–7745.

645 50. Rudolph RE, Sams C, Steiner R, Thomas SH, Walker S, Uchanski ME. 2015. Biofumigation
646 performance of four brassica crops in a green chile pepper (Capsicum annuum) rotation
647 system in southern New Mexico. HortScience 50:247–253.

648 51. Ranjan VK, Mukherjee S, Thakur S, Gupta K, Chakraborty R. 2021. Pandrug-resistant
649 Pseudomonas sp. expresses New Delhi metallo-β-lactamase-1 and consumes ampicillin as
650 sole carbon source. Clin Microbiol Infect 27:472.e1-472.e5.

651 52. Smith BJ, Kirkegaard JA. 2002. In vitro inhibition of soil microorganisms by 2-phenylethyl
652 isothiocyanate. Plant Pathol 51:585–593.

653 53. Yun Y-K, Kim H-K, Kim J-R, Hwang K, Ahn Y-J. 2012. Contact and fumigant toxicity of
654 *Armoracia rusticana* essential oil, allyl isothiocyanate and related compounds to
655 *Dermatophagoides farinae*. Pest Manag Sci 68:788–794.

656 54. Bainard LD, Brown PD, Upadhyaya MK. 2009. Inhibitory Effect of Tall Hedge Mustard (
657 *Sisymbrium loeselii*) Allelochemicals on Rangeland Plants and Arbuscular Mycorrhizal Fungi.
658 Weed Sci 57:386–393.

659 55. Kurt Ş, Güneş U, Soylu EM. 2011. *In vitro* and *in vivo* antifungal activity of synthetic pure
660 isothiocyanates against *Sclerotinia sclerotiorum*. Pest Manag Sci 67:869–875.

661 56. Matthiessen JN, Shackleton MA. 2005. Biofumigation: environmental impacts on the
662 biological activity of diverse pure and plant-derived isothiocyanates. Pest Manag Sci 61:1043–
663 1051.

664 57. Vaughn SF, Palmquist DE, Duval SM, Berhow MA. Herbicidal Activity of Glucosinolate-
665 Containing Seedmeals.

666 58. Manici LM, Lazzeri L, Palmieri S. 1997. In Vitro Fungitoxic Activity of Some Glucosinolates and
667 Their Enzyme-Derived Products toward Plant Pathogenic Fungi. J Agric Food Chem 45:2768–
668 2773.

669 59. Neubauer C, Heitmann B, Müller C. 2014. Biofumigation potential of Brassicaceae cultivars to
670 Verticillium dahliae. Eur J Plant Pathol 140:341–352.

671 60. Loewe L, Textor V, Scherer S. 2003. High Deleterious Genomic Mutation Rate in Stationary
672 Phase of Escherichia coli. Science (80-) 302:1558–1560.

673 61. Navarro Llorens JM, Tormo A, Martínez-García E. 2010. Stationary phase in gram-negative
674 bacteria. FEMS Microbiol Rev. Blackwell Publishing Ltd.

675 62. Olsen I. 2015. Biofilm-specific antibiotic tolerance and resistance. Eur J Clin Microbiol Infect
676 Dis. Springer Verlag.

677 63. Murakami K, Ono T, Viducic D, Kayama S, Mori M, Hirota K, Nemoto K, Miyake Y. 2005. Role
678 for rpoS gene of Pseudomonas aeruginosa in antibiotic tolerance. FEMS Microbiol Lett
679 242:161–167.

680 64. Knöppel A, Näsvall J, Andersson DI. 2017. Evolution of antibiotic resistance without antibiotic
681 exposure. Antimicrob Agents Chemother 61:1495–1512.

682 65. Zampieri M, Enke T, Chubukov V, Ricci V, Piddock L, Sauer U. 2017. Metabolic constraints on
683 the evolution of antibiotic resistance. Mol Syst Biol 13:917.

684 66. Marshall CG, Zolli M, Wright GD. 1999. Molecular mechanism of VanHst, an α-ketoacid

685 dehydrogenase required for glycopeptide antibiotic resistance from a glycopeptide producing
686 organism. Biochemistry 38:8485–8491.

687 67. Lee YH, Kingston AW, Helmann JD. 2012. Glutamate dehydrogenase affects resistance to cell
688 wall antibiotics in Bacillus subtilis. J Bacteriol 194:993–1001.

689 68. Lacour S, Bechet E, Cozzone AJ, Mijakovic I, Grangeasse C. 2008. Tyrosine Phosphorylation of
690 the UDP-Glucose Dehydrogenase of Escherichia coli Is at the Crossroads of Colanic Acid
691 Synthesis and Polymyxin Resistance. PLoS One 3:e3053.

692 69. Rodionova IA, Zhang Z, Aboulwafa M, Saier MH. 2020. UDP-glucose dehydrogenase Ugd in E.
693 coli is activated by Gmd and RffD, is inhibited by CheY, and regulates swarming. bioRxiv.
694 bioRxiv.

695 70. Beltramini AM, Mukhopadhyay CD, Pancholi V. 2009. Modulation of cell wall structure and
696 antimicrobial susceptibility by a Staphylococcus aureus eukaryote-like serine/threonine
697 kinase and phosphatase. Infect Immun 77:1406–1416.

698 71. Pasternak C, Dulermo R, Ton-Hoang B, Debuchy R, Siguier P, Coste G, Chandler M, Sommer S.
699 2013. IS *Dra 2* transposition in *D einococcus radiodurans* is downregulated by TnpB. Mol
700 Microbiol 88:443–455.

701 72. Lopatkin AJ, Bening SC, Manson AL, Stokes JM, Kohanski MA, Badran AH, Earl AM, Cheney NJ,
702 Yang JH, Collins JJ. 2021. Clinically relevant mutations in core metabolic genes confer
703 antibiotic resistance. Science (80-) 371.

704 73. Wistrand-Yuen E, Knopp M, Hjort K, Koskiniemi S, Berg OG, Andersson DI. 2018. Evolution of
705 high-level resistance during low-level antibiotic exposure. Nat Commun 9:1–12.

706 74. Baym M, Lieberman TD, Kelsic ED, Chait R, Gross R, Yelin I, Kishony R. 2016. Spatiotemporal
707 microbial evolution on antibiotic landscapes. Science (80-) 353:1147–1151.

708 75. Kumar S, Trivedi PK. 2018. Glutathione S-transferases: Role in combating abiotic stresses
709 including arsenic detoxification in plants. Front Plant Sci. Frontiers Media S.A.

710 76. Rahmanpour S, Backhouse D, Nonhebel HM. 2009. Induced tolerance of *Sclerotinia*
711 *sclerotiorum* to isothiocyanates and toxic volatiles from *Brassica* species. Plant Pathol
712 58:479–486.

713 77. Calmes B, N'Guyen G, Dumur J, Brisach CA, Campion C, Lacomi B, PignÉ S, Dias E, Macherel D,
714 Guillemette T, Simoneau P. 2015. Glucosinolate-derived isothiocyanates impact
715 mitochondrial function in fungal cells and elicit an oxidative stress response necessary for
716 growth recovery. Front Plant Sci 6:414.

717 78. Wu J, Kong HG, Jung EJ, Choi SY, Lee HJ, Tao W, Chung E, Lee SW. 2015. Loss of glutamate
718 dehydrogenase in Ralstonia solanacearum alters dehydrogenase activity, extracellular
719 polysaccharide production and bacterial virulence. Physiol Mol Plant Pathol 90:57–64.

720 79. Back M, Barker A, Evans K. 2019. Effectiveness of biofumigant crops for the management of
721 PCN in GB. Agricultural And Horticultural Development Board (AHDB).

722 80. Hanschen FS, Brü N, Brodehl A, Mewis I, Schreiner M, Rohn S, Kroh LW. 2012.
723 Characterization of Products from the Reaction of Glucosinolate-Derived Isothiocyanates with
724 Cysteine and Lysine Derivatives Formed in Either Model Systems or Broccoli Sprouts
725 https://doi.org/10.1021/jf301718g.

726 81. Seemann T. 2014. Prokka: rapid prokaryotic genome annotation. Bioinformatics 30:2068–
727 2069.

728 82. Guarischi-Sousa R, Puigvert M, Coll NS, Siri MI, Pianzzola MJ, Valls M, Setubal JC. 2016.
729 Complete genome sequence of the potato pathogen Ralstonia solanacearum UY031. Stand
730 Genomic Sci 11:7.

731 83. Arndt D, Grant JR, Marcu A, Sajed T, Pon A, Liang Y, Wishart DS. 2016. PHASTER: a better,
732 faster version of the PHAST phage search tool. Nucleic Acids Res 44:W16–W21.

733 84. Durrant MG, Li MM, Siranosian BA, Montgomery SB, Bhatt AS. 2020. A Bioinformatic Analysis
734 of Integrative Mobile Genetic Elements Highlights Their Role in Bacterial Adaptation. Cell
735 Host Microbe 27:140-153.e9.

736

737 ## Figures and figure legends

A

Isothiocyanate	IUPAC name	Molar mass (g mol^{-1})	Structure
Allyl	3-isothiocyanato-1-propene	99.15	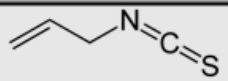
Sec-Butyl	2-isothiocyanatobutane	115.19	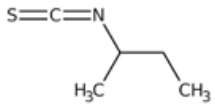
2-Phenylethyl (PEITC)	(2-Isothiocyanatoethyl) benzene	163.24	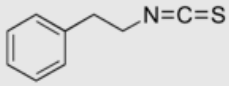

B

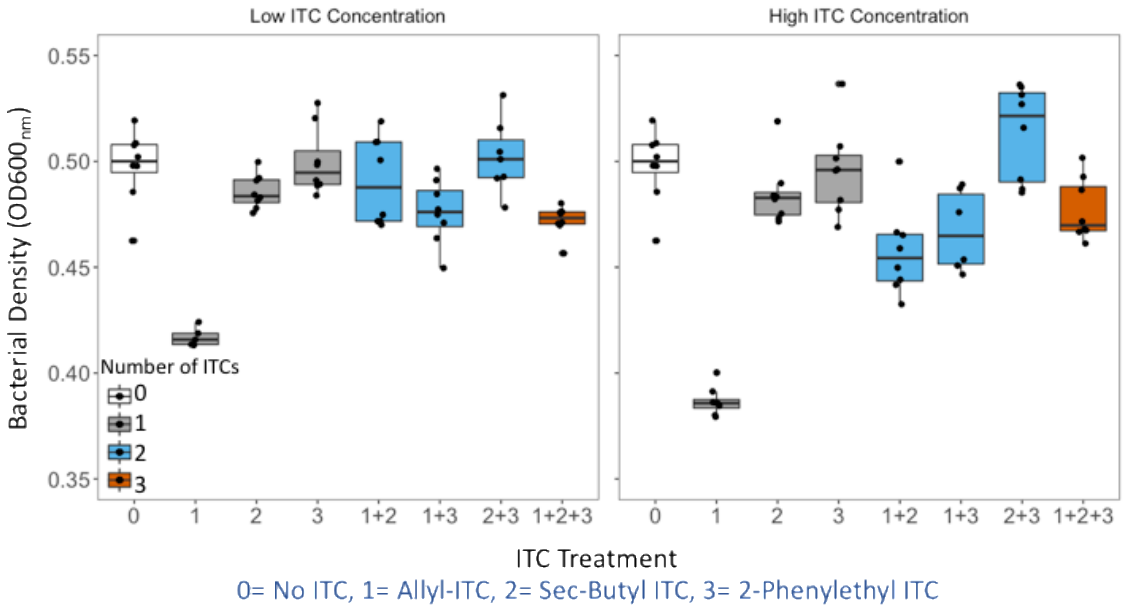

738

739 **Figure 1. The antimicrobial activity of different ITCs against *Ralstonia solanacearum***

740 **pathogen when applied alone and in combination.** The chemical properties of the three

741 different ITCs predominantly released from Indian mustard biofumigant plant (*Brassica*

742 *juncea*) (A), and their effects on *R. solanacearum* growth after 48h exposure when applied

743 alone and in combination in liquid microcosms at low (500 μM) and high (1000 μM)

744 concentrations (B). In (B) boxplot colours represent different ITC treatments that are

745 labelled on X-axes as follows: (0): non-ITC exposed (control); (1) allyl-ITC; (2) sec-butyl ITC

746 and (3) 2-phenylethyl ITC. Individual data points show bacterial densities for each technical

747 replicate (N= 8). The boxplots show the minimum, maximum, interquartile range and the

748 median (black line).

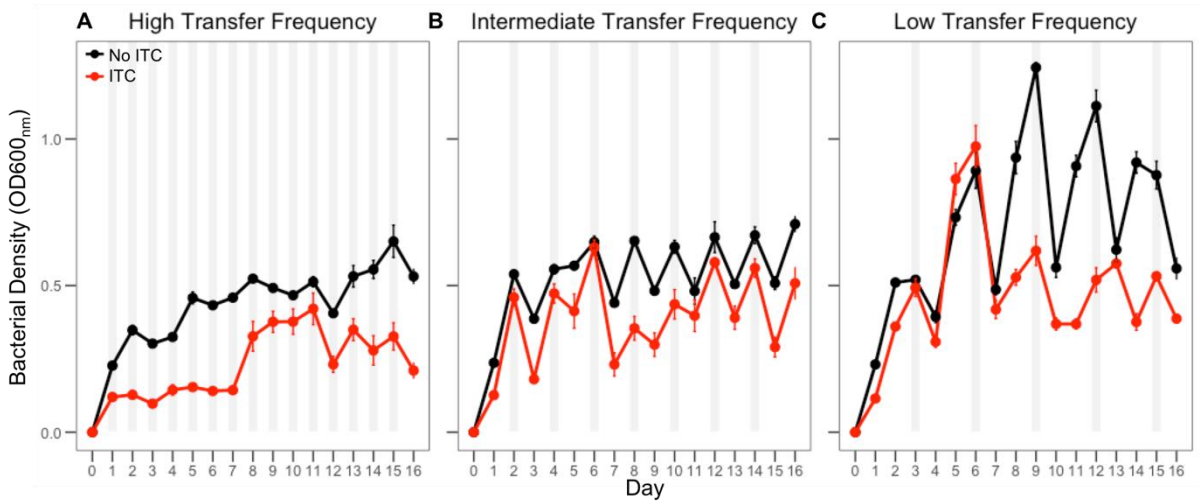

Figure 2. *Ralstonia solanacearum* density dynamics ($OD600_{nm}$) during the evolution experiment in the absence and presence of allyl-ITC in high, intermediate and low transfer frequency treatments. In all panels, black and red lines correspond to *R. solanacearum* densities in the absence and presence of 500 μM allyl-ITC, respectively. Panels A-C correspond to high (1-day), intermediate (2-day) and low (3-day) transfer frequency treatments, respectively. Grey shaded areas indicate the time point of serial transfers, while optical density reads were taken at 24-hour intervals in all treatments. Each time point shows the mean of eight biological replicates and bars show ±1 error of mean.

758

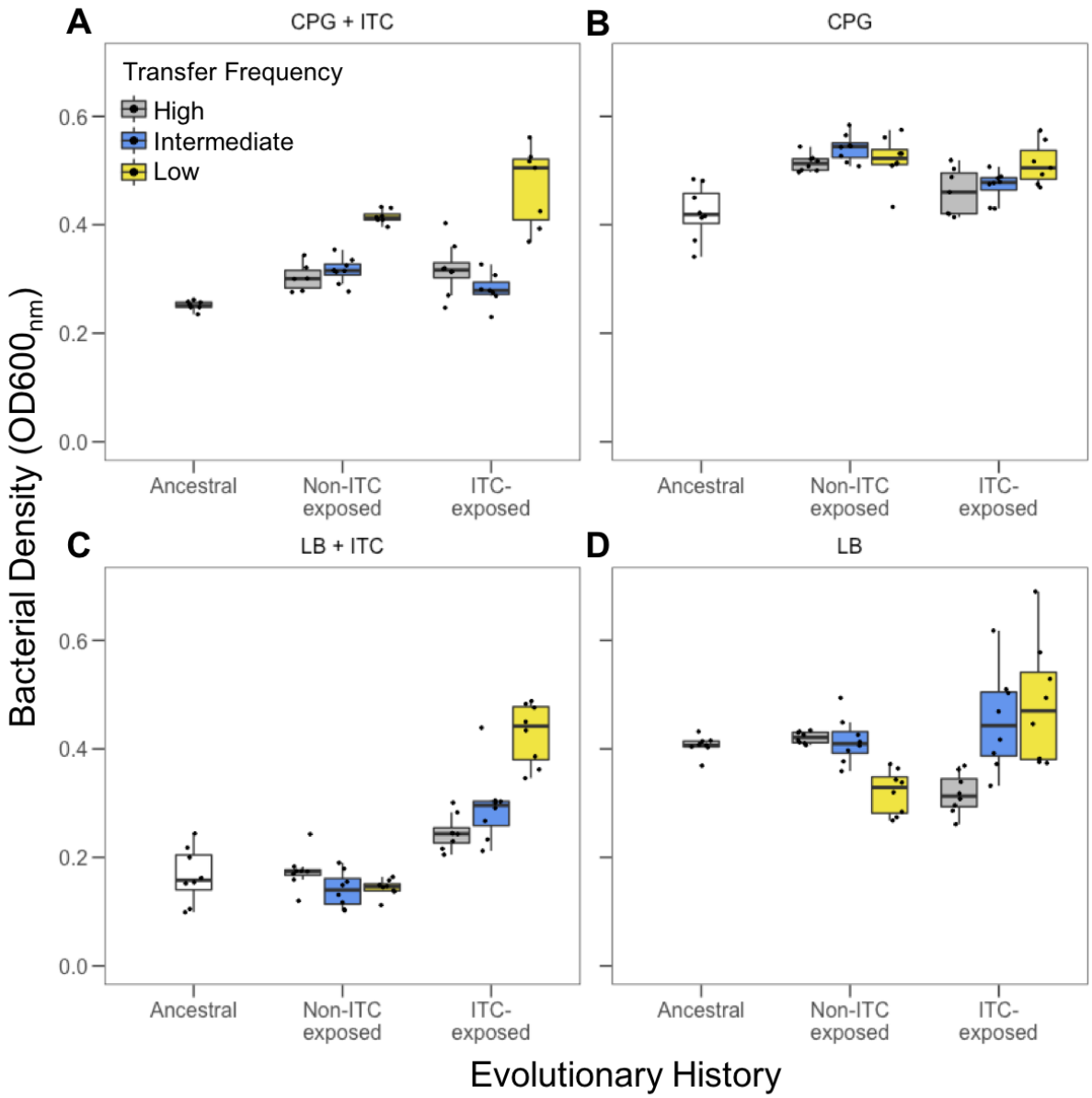

759

760 **Figure 3. Comparison of *Ralstonia solanacearum* ITC tolerance between the ancestral**

761 **clone and evolved populations from high, intermediate and low transfer frequency**

762 **treatments at the end of the evolution experiment in CPG and LB media.** ITC tolerance was

763 determined as *R. solanacearum* growth ($OD600_{nm}$) after 48 hours of exposure to 500 μM

764 allyl-ITC in CPG (A) and LB (C) media. Growth was also measured in the absence of allyl-ITC

765 in both CPG (B) and LB (D) media. High (1-day), intermediate (2-day) and low (3-day)

766 transfer frequency treatments are shown in grey, blue and yellow boxplots, respectively,
767 and boxplots show the minimum, maximum, interquartile range and the median (black line).
768 Individual data points show bacterial densities for each biological replicate population (N=
769 8).

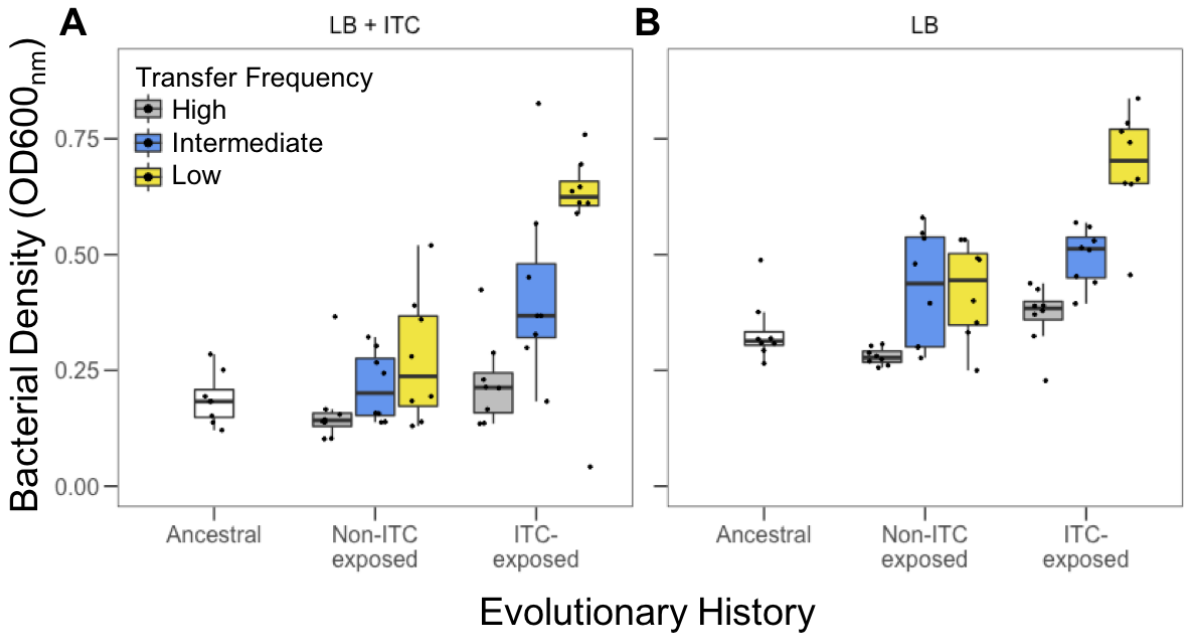

770

771 **Figure 4. Comparison of *Ralstonia solanacearum* ITC tolerance between the ancestral and**
772 **evolved clones from high, intermediate and low transfer frequency treatments at the end**
773 **of the evolution experiment in LB media.** ITC tolerance was determined as *R. solanacearum*
774 growth ($OD600_{nm}$) after 48 hours of exposure to 500 μM allyl-ITC in LB media (A). Growth
775 was also measured in the absence of allyl-ITC (B). High (1-day), intermediate (2-day) and low
776 (3-day) frequency treatments are shown in grey, blue and yellow, respectively, and boxplots
777 show the minimum, maximum, interquartile range and the median (black line). Individual
778 data points show bacterial densities for each biological replicate population (N= 8).

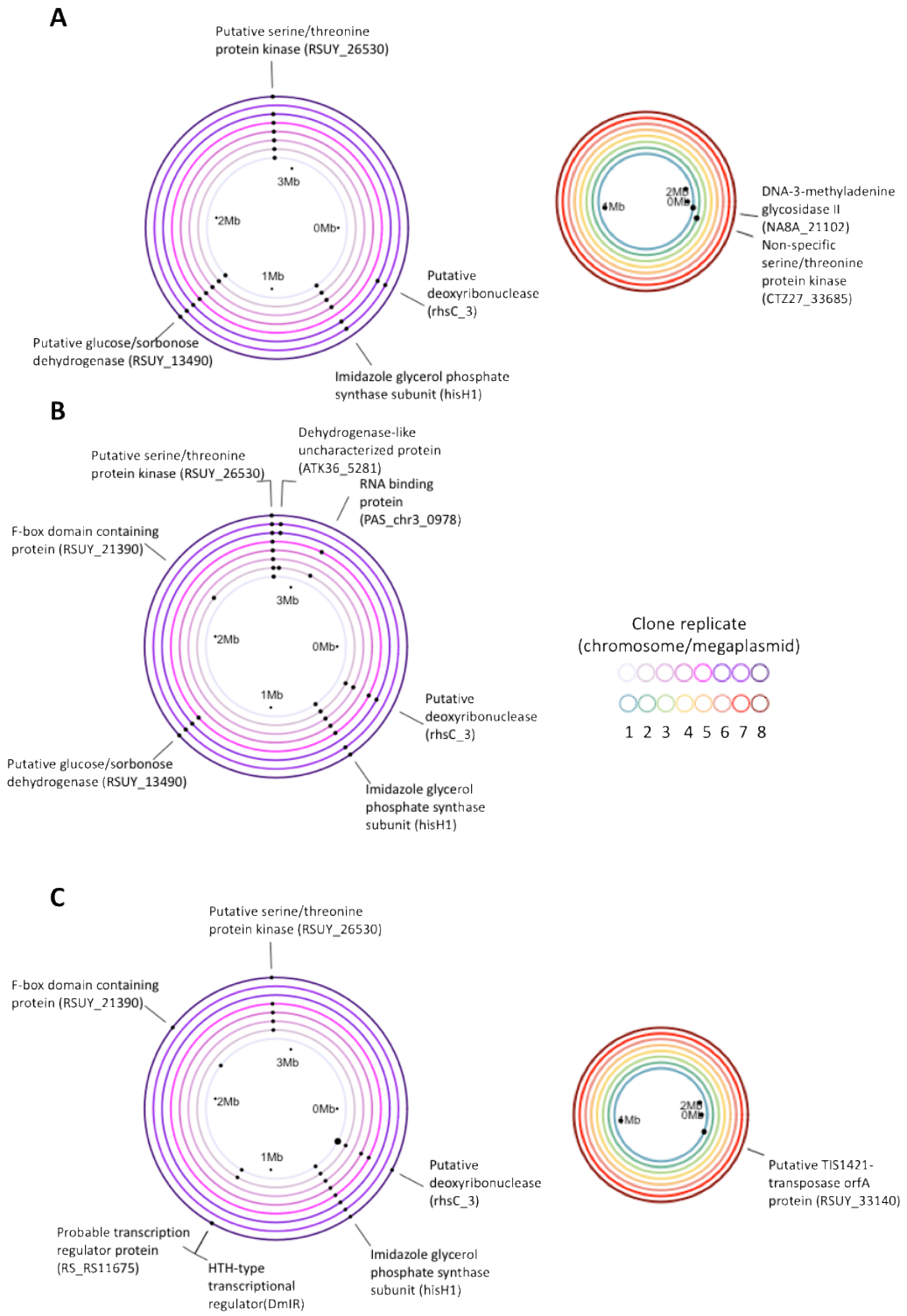

Figure 5. Mutations associated with evolved *Ralstonia solanacearum* clones. In each panel, each ring represents a replicate *R. solanacearum* clone in different colours (N= 8, see key). Panels show replicate clones isolated from low transfer frequency ITC-exposure treatment (A), low transfer frequency control treatment (B) and intermediate transfer frequency

784 control treatment (C). Circles on the left and right show mutations identified in chromosome
785 and megaplasmid, respectively (see key), and black dots on the rings represent mutations at
786 different loci. Labels indicate the gene product and the locus tag or gene name. Within each
787 ring is a distance marker in Mb.

788 ## Supplementary Materials

789 **Supplementary Table 1. The mean density reduction (%) of *Ralstonia solanacearum***
790 **bacterium when exposed to 500 or 1000 µM allyl, sec-butyl and 2-phenylethyl ITCs in CPG**
791 **growth media after 24, 48 or 72 hours relative to when grown in the absence of ITCs.** This
792 table is based on the same data presented in Supplementary Fig. 2.

ITC Type and Concentration (µM)	Time (h)	Bacterial density reduction (%) compared to control
Allyl-ITC, 500	24	66
	48	54
	72	27
Allyl-ITC, 1000	24	66
	48	47
	72	41
Sec-Butyl ITC, 500	24	33
	48	26
	72	9
Sec-Butyl ITC, 1000	24	30
	48	27
	72	8
2-Phenylethyl ITC, 500	24	39
	48	13
	72	10
2-Phenylethyl ITC, 1000	24	38
	48	18
	72	13

793

794 **Supplementary Table 2. Mutated *Ralstonia solanacearum* genes and annotated gene functions observed in intermediate and low transfer**

795 **frequency control (no-ITC), and ITC-exposed low transfer frequency treatments.** Gene function predictions were derived based on BLAST

796 using UNIPROT and percentage (%) sequence similarity is included for putative (hypothetical) proteins. Filled cells denote for the presence of

797 mutations in given clones and white cells denote for the absence of given mutations.

Location	Chromosome	Chromosome	Chromosome	Chromosome	Chromosome	Chromosome	Chromosome	Chromosome	Chromosome	Chromosome	Plasmid	Plasmid	Plasmid
Position	293900	294413	585646	1257034	1258240	1449567	2302809	2830656	2874048	3123064	44512	105610	124931
Type	snp	snp	ins	snp	snp	snp	snp	ins	ins	ins	del (27bp)	del (1bp)	snp
Ref	G	C	T	G	C	C	C	A	C	A	TCGTGAGCGGCAAGCCGGCACATCGCAA	TG	G
Alt	A	T	TCGTGCTG	C	G	T	T	ACAGCAACGG	CGGGCACT	AC	T	T	A
Effect	Synonymous variant	Synonymous variant	Frameshift variant	Missense variant	Missense variant	Missense variant	Synonymous variant	Conservative inframe insertion	Frameshift variant	Conservative inframe insertion	Frameshift variant	Synonymous variant	Missense variant
Locus tag	RSUY_02640	RSUY_02640	RSUY_05230	RSUY_11710	RS_RS11675	RSUY_13490	RSUY_21390	RSUY_26530	ATK36_5281	PAS_chr3_0978	NA8A_21102	CTZ27_33685	RSUY_33140
Product	Putative deoxyribonuclease RhsC	Putative deoxyribonuclease RhsC	Imidazole glycerol phosphate synthase subunit HisH1	HTH-type transcriptional regulator DmlR	Probable transcription regulator protein (86.1% similarity)	Putative glucose/sorbonose dehydrogenase (84.8% similarity)	F-box domain-containing protein (83.3% similarity)	Putative serine/threonine protein kinase (91.7% similarity)	Dehydrogenase-like uncharacterised protein (90.9% similarity)	RNA binding protein (90.9% similarity)	DNA-3-methyladenine glycosidase II (100% similarity)	Non-specific serine/threonine protein kinase (91.7% similarity)	Putative TIS1421-transposase orfA protein (72.7% similarity)
Int No ITC 1													
Int No ITC 2													
Int No ITC 3													
Int No ITC 4													
Int No ITC 5													
Int No ITC 6													
Int No ITC 7													
Int No ITC 8													
Low No ITC 1													
Low No ITC 2													
Low No ITC 3													
Low No ITC 4													
Low No ITC 5													
Low No ITC 6													
Low No ITC 7													
Low No ITC 8													
Low ITC 1													
Low ITC 2													
Low ITC 3													
Low ITC 4													
Low ITC 5													
Low ITC 6													
Low ITC 7													
Low ITC 8													

798

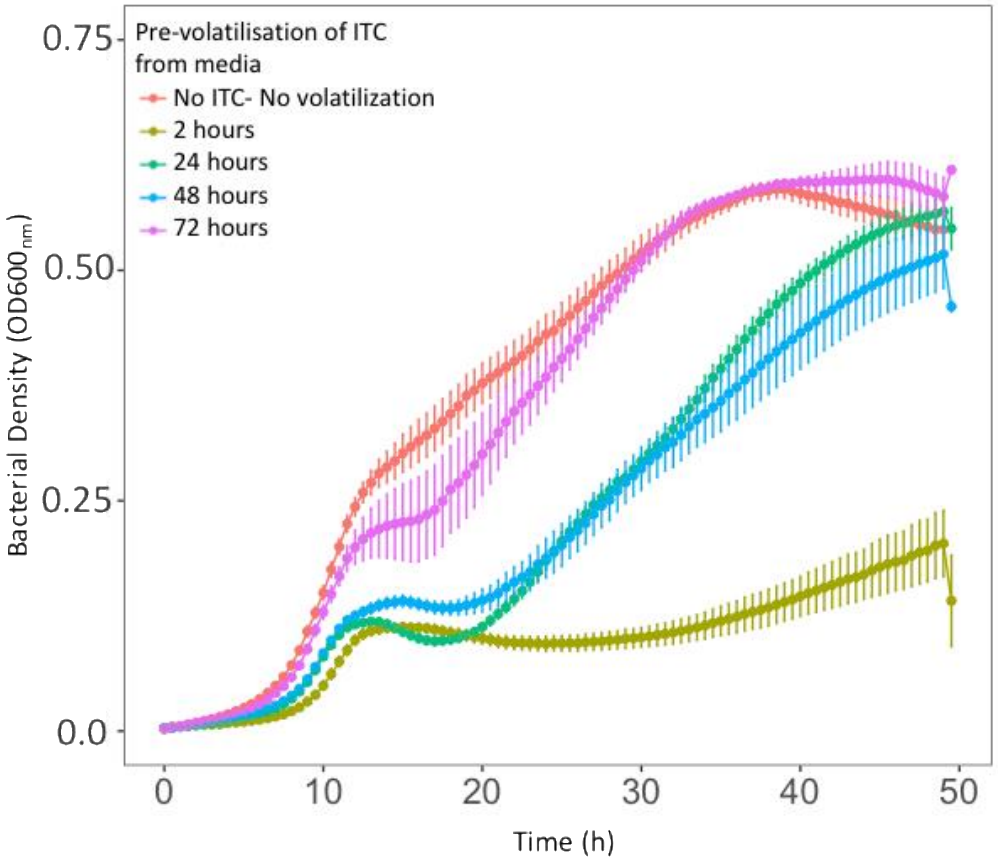

Supplementary Figure. 1. The effect of allyl-ITC pre-volatilisation for antibacterial activity against *Ralstonia solanacearum*. *R. solanacearum* bacterial growth was measured in CPG media supplemented with 0 (No allyl-ITC) or 500 μM of allyl-ITC that had been allowed to volatilise for 2, 24, 48 or 72 hours (see key). All data points show the mean of eight technical replicates and bars show ±1 standard error of the mean (SEM).

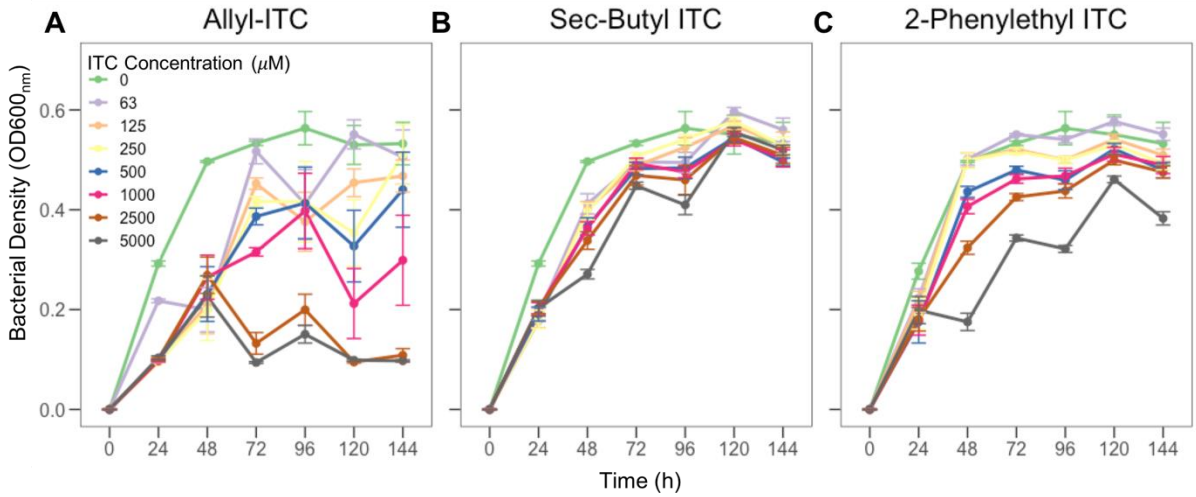

806

807 **Supplementary Figure 2. Effects of allyl, sec-butyl and 2-phenylethyl ITCs on *Ralstonia***

808 ***solanacearum* growth at different ITC concentrations.** In all panels, *R. solanacearum*

809 bacterial densities are shown on the Y-axis as optical density ($OD600_{nm}$), measured at 24-

810 hour intervals (X-axis). In all panels, different line colours refer to different ITC

811 concentrations (see key in A). All data points show the mean of eight technical replicates

812 and bars show ±1 standard error of the mean (SEM).

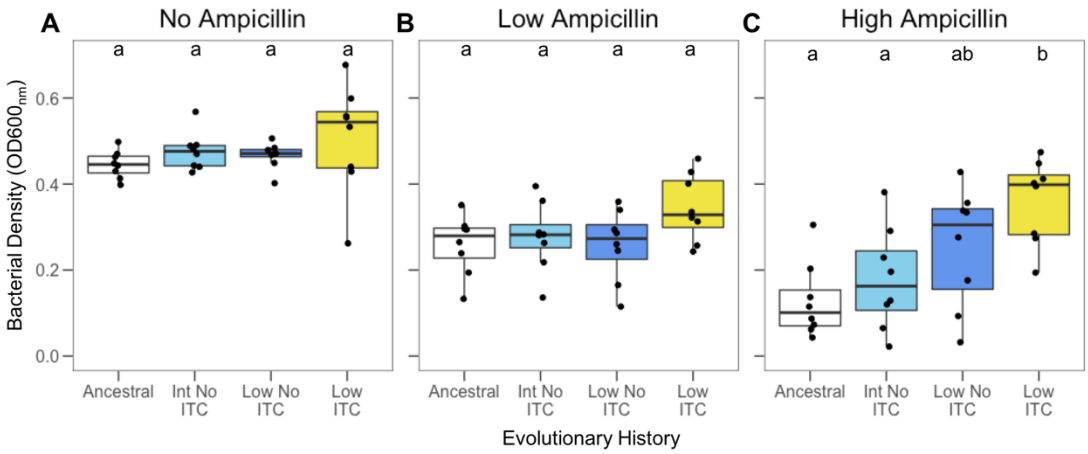

Supplementary Figure 3. *Ralstonia solanacearum* tolerance to ampicillin beta-lactam antibiotic. Ampicillin tolerance was measured as the growth of ancestral and evolved *R. solanacearum* clones isolated from intermediate (Int) and low transfer frequency (Low) control treatments (no-ITC) and ITC-exposed low transfer frequency treatment in the absence (A) and presence (B-C) of ampicillin (15 and 30 µg/ml concentrations). Boxplots show the minimum, maximum, interquartile range and the median (black line) after 48 hours. Individual data points show bacterial densities for each biological replicate clone (N= 8). Different small case letters above boxplots indicate significant pairwise differences (Tukey: $p < 0.05$) between treatments within each panel.